Ecological Indicators 69 (2016) 522–532

Contents lists available at ScienceDirect

Ecological Indicators

journal homepage: www.elsevier.com/locate/ecolind

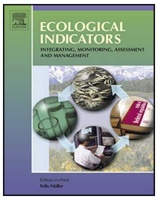

An ostracod-based calibration function for electrical conductivity reconstruction in lacustrine environments in Patagonia, Southern South America

Josefina Ramón Mercau*, Cecilia Laprida

Instituto de Estudios Andinos "Don Pablo Groeber" (UBA-CONICET), Intendente Güiraldes 2160 (Ciudad Universitaria), 1428 Buenos Aires, Argentina

ARTICLE INFO

Article history:
Received 22 December 2015
Received in revised form 13 May 2016
Accepted 15 May 2016

Keywords:
Quantitative salinity reconstruction
Transfer function
Holocene
Ostracoda
Paleohydrology
Closed lakes

ABSTRACT

In the Patagonian region (~37–56°S) E of the Andes, the salinity and solute composition of lakes is strongly related to their location along the marked W-E decreasing precipitation gradient that is one of the main climatic features of the area. A calibration function ($n = 34$) based on 12 ostracod species (Ostracoda, Crustacea) was developed by WA-PLS to quantitatively reconstruct electrical conductivity (EC) values as a salinity proxy. The selected one component model had a $r^2 = 0.74$ and RMSEP and maximum bias equal to 16% and 31% of the sampled range, respectively, comparable to other published ostracod-based calibration functions. This model was applied to the ostracod record of the closed lake Laguna Cháltel (49°58′S, 71°07′W), comprising seven species and dominated by two species of the genus *Limnocythere*. In order to evaluate the calibration function's robustness, the obtained EC values were compared with qualitative lake level and salinity variations inferred through a multiproxy hydrological reconstruction of the lake. Both reconstructions show good overall agreement, with reconstructed EC values in the oligo-mesohaline range (average: 11 060 ± 680 μS/cm) between 4570 and 3190 cal BP, corresponding to the ephemeral and shallow lake phases, and a marked decrease in EC concurrent with a lake level rise, reaching an average EC of 1140 ± 90 μS/cm during the deep lake phase (1720 cal BP to present). The variability in the reconstructed EC values for the ephemeral lake phase showed some inconsistency with the expected trend, which was attributed to time-averaging effects; for its part, the pace of the decrease in EC during the medium-depth phase (3190–1720 cal BP) differed from the expected, which could be due to autigenic effects (redissolution of salts) at the onset of this phase. This comparison not only lends support to the adequacy of the calibration function, but also suggests that its application in the context of a multiproxy study can greatly contribute to distinguish between autigenic and climatic-related controls of paleosalinity in closed lakes, allowing performing more accurate paleoenvironmental inferences on the basis of paleohydrological reconstructions.

1. Introduction

During the last decades, the need to contextualize major environmental processes such as acidification, eutrophication and climate change within the natural variability of the ecological and climatic systems has promoted the development of numerous approaches and techniques for paleoenvironmental reconstruction. Lake sediments, whose origin, composition and deposition are strongly influenced by climatically-controlled processes, constitute good archives of past climatic and environmental conditions, which can be analysed through the use of sedimentary components and characteristics as proxies (Smol et al., 2012). In particular, abiotic variables can be reconstructed based on the study of fossil biotic components of past ecosystems. Quantitative paleoenvironmental inferences can be achieved through the application of appropriate numerical techniques, such as the widely used multivariate calibration functions (CF), also known as transfer functions (Birks et al., 2010).

While a wealth of quantitative paleoenvironmental reconstructions has been published since the 1980s, the Southern Hemisphere and particularly South America is underrepresented in this effort with respect to its Northern counterpart. In particular, and despite its great interest for paleoclimatic reconstruction as the sole continental landmass entirely within the area of influence of the Southern Westerly Wind (SWW) belt (Kilian and Lamy, 2012), to

---

* Corresponding author.
E-mail addresses: jrm@gl.fcen.uba.ar (J. Ramón Mercau), chechu@gl.fcen.uba.ar (C. Laprida).

http://dx.doi.org/10.1016/j.ecolind.2016.05.026
1470-160X/

date only five CF have been published for continental southern South America (Patagonia): two pollen-based CF for precipitation estimation (Tonello et al., 2009; Schäbitz et al., 2013); one chironomid-based CF for air temperature estimation (Massaferro and Larocque-Tobler, 2013); one thecamoebian-based CF for water table depth reconstruction in peat bogs (Van Bellen et al., 2014), and an ostracod-based CF for chlorine content estimation (Cusminsky et al., 2011).

Ostracods (Crustacea: Ostracoda) are aquatic organisms widely distributed throughout continental and marine environments. They secrete calcite bivalved carapaces with high preservation potential in sediments and rocks, which, coupled with their sensitivity to specific environmental conditions, render them advantageous proxies. Indeed, ostracods were among the first biological proxies to be used to draw quantitative inferences of environmental parameters (Delorme, 1971). Several continental ostracods species show marked preferences for specific water types, in terms of solute concentration (salinity) and ionic composition (e.g., De Deckker, 2002). Accordingly, most of the ostracod-based calibration functions for continental environments published to date (for a review, see Viehberg and Mesquita-Joanes, 2012) estimate salinity-related variables such as electrical conductivity (EC) or the concentration of a major ion.

To the best of our knowledge, to date only four ostracod-based CF for reconstruction of salinity-related variables have been published for the Southern Hemisphere: two for Australia (Gouramanis et al., 2010; Kemp et al., 2012) and two for South America, specifically the Bolivian Altiplano (Mourguiart and Roux, 1990) and Patagonia (Cusminsky et al., 2011). The latter, as already mentioned, was applied to the ostracod record of Lake Cardiel (49°S, 71°W) to reconstruct chlorine content concentration, but neither the calibration set nor any model parameters or performance indicators were presented, which precludes comparison with the present CF. Other than this reference, no quantitative salinity-related estimation models, based on ostracods or otherwise, have been published so far for continental Patagonia.

Fluctuations in the salinity and lake level of closed lakes in arid and semi-arid regions have been long recognized as sensitive indicators of change in the precipitation to evaporation ratio (P/E) (e.g., Gasse et al., 1997). During dry periods evaporation exceeds water input, causing lake level to fall and ion concentration to increase; this process is affected by hydrological and morphometric features of the lakes and their watersheds, as well as lake water geochemistry (Fritz et al., 1991). In this context, ostracods from these environments can be valuable (paleo)hydrological indicators.

Patagonian lakes have been shown to vary in their major ion concentration and composition in a manner that can be related with their location within the marked West-East precipitation gradient that constitutes one of the most characteristic features of Patagonian climate east of the Andes. While the lakes located in the wetter part of the gradient present bicarbonate-dominated waters of low EC, those receiving a much lower precipitation input have high EC and present sodium-dominated waters enriched in all major anions, indicative of evaporative conditions (Baigún and Marinone, 1995; Díaz et al., 2007; Ramón Mercau et al., 2012). These distinct water types, in turn, are inhabited by different ostracod species; their marked hydrochemical preferences make it possible to use these taxa as semi-quantitative paleohydrological indicators (i.e., for the qualitative estimation of host water salinity range and major ion composition) (Ramón Mercau et al., 2012). This approach was successfully applied to the ostracod record of the volcanic crater lake Laguna Cháltel (49°58′S, 71°07′W, southern Patagonia) in the context of a multi-proxy study to reconstruct the hydrological changes that took place in it during the last 4600 years (Ohlendorf et al., 2014).

In the present contribution, we built on the hydrochemical preferences previously inferred for Patagonian ostracods (Ramón Mercau et al., 2012), incorporating new data on ostracod assemblage composition and EC of samples from Southern and Central Patagonian lakes in order to generate a calibration function for quantitative reconstruction of EC as a proxy for salinity. The calibration function obtained was applied to the Laguna Cháltel ostracod record to reconstruct past EC values of the lake. The results obtained were compared with the reconstructed lake level variations and salinity shifts inferred from several independent proxies by Ohlendorf et al. (2014), in order to assess the reliability of the ostracod-based reconstruction.

2. Study area

2.1. Regional setting and climate

The Patagonian region is located in the southernmost part of South America, between 37°S and 56°S approximately (Fig. 1a). It can be divided into two distinct subregions: the Andean Patagonia to the west, comprising the Andean Cordillera, and the Patagonian Steppe to the east, characterized by extensive tablelands (Coronato et al., 2008). The mountain range acts as a barrier to the flux of the SWW, or westerlies, which carry moist air from the Pacific Ocean; this causes abundant orographic precipitation over the windward (west) side of the Cordillera and a major rainshadow effect on its leeward (east) side. As a result, in the Argentinean Patagonia there is a dramatic West-East mean annual precipitation gradient that decreases from ca. 1400 mm in the Andean range to less than 200 mm in the steppe (Paruelo et al., 1998; Garreaud et al., 2013). During Austral summer, the westerlies are centred between 45°S–55°S and present higher intensity, while in Austral winter the wind belt migrates northward and weakens at lower levels. The seasonality of precipitations in the Eastern side of Patagonia, with a clearly defined rainy season during Austral winter, is highly correlated to this seasonal shift of the westerlies (Garreaud et al., 2013). With regards to temperature, Patagonia can be considered a temperate to cool-temperate region, with mean annual temperature ranging from 12 °C in the northeast to 3 °C in the southwest. Mean thermal amplitude exhibits a similar NE-SW decrease, varying between 16 °C and 5 °C (Paruelo et al., 1998).

2.2. Laguna Cháltel

The analysed sedimentary sequence was obtained from the crater lake Laguna Cháltel, located on a volcanic plateau at 788 m.a.s.l. in the province of Santa Cruz, Argentina (Fig. 1b). Its remote steppe location suggests low mean annual precipitations, although as Ohlendorf et al. (2014) note, its high elevation could account for locally moister conditions, as implied by local oral reports of abundant snow during winter in the plateau. The 41 m-deep lake is almost circular in shape, with the western side of the basin presenting a more pronounced slope than the eastern side (Fig. 1c). It presents three small inflows of unknown temporal stability, and no outlets. Water chemistry on the Austral summer of 2004 (2004-03-09) was characterized by dominance of carbonate and sodium; EC presented little variability throughout the water column, with a mean value of 788 μS/cm (Ohlendorf et al., 2014). On the Austral autumn of 2013 (2013-04-05), the lake presented a similar hydrochemistry, with an EC of 815 μS/cm and Na-Mg-HCO_3 ionic composition (Christoph Mayr, pers. comm.).

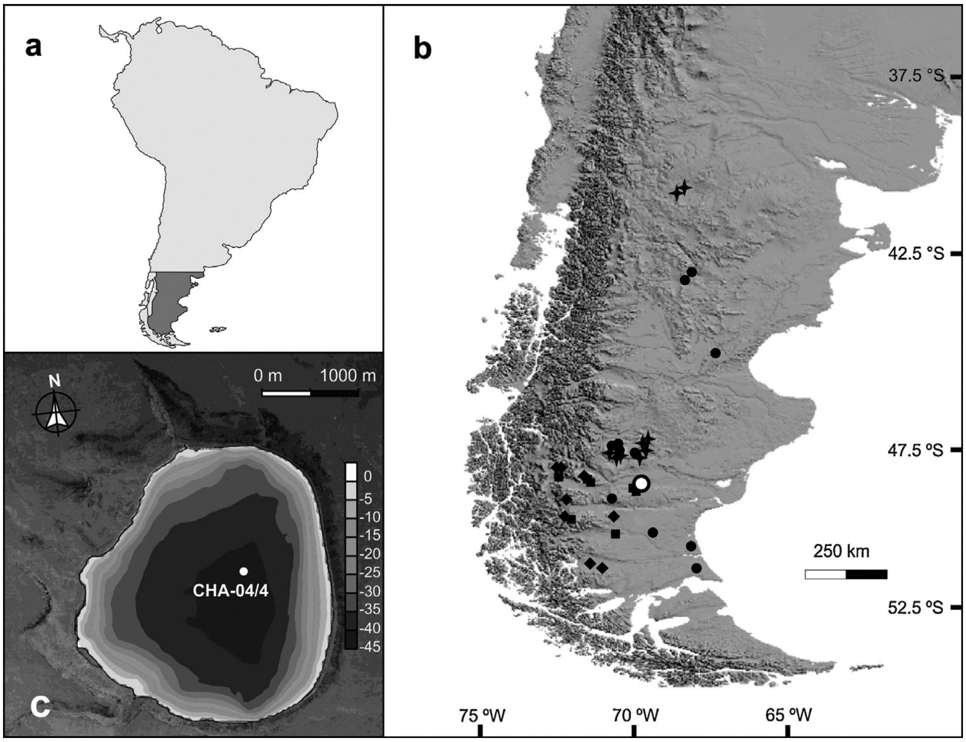

Fig. 1. Location map of (a) the approximate limits of the studied Patagonian region, E of the Andean Cordillera and (b) the sampled lakes (Subset 1: filled squares; Subset 2: filled circles; Subset 3: filled diamonds; Subset 4: filled stars) and Laguna Cháltel (empty circle), together with (c) the bathymetry of Laguna Cháltel. (b) Modified after Ramón Mercau et al. (2012); (c) modified after Ohlendorf et al. (2014).

3. Materials and methods

3.1. Calibration set

The samples included in the present ostracod-EC calibration set were obtained in the course of different investigations; a total of four subsets of samples were included (Table A1).

Several paired water and surface sediment samples were obtained during a field trip carried out in March-April 2013 in Southern Patagonia between 49°–52°S and 69°–73°W approximately. They are part of a larger set collected for a study whose purpose was to investigate the relations between isotopic compositions of host water and sedimentary biogenic compounds (Mayr et al., 2015). Water and sediment sampling methods, as well as ostracods extraction, are described in Mayr et al. (2015). A total of 11 samples, herein referred to as Subset 1, were taken into account for the present contribution.

Subset 2 consisted of 15 plankton-net samples, which were screened for ostracods. These were obtained from shallow lakes within the framework of different research projects and kindly loaned for the present contribution by one of the researchers, MSc. María Cristina Marinone. Only samples from shallow lakes were used, as it was considered that in such cases the benthic community was being sampled by the sweep of the net throughout the water column, as evidenced by the presence of other epibenthic invertebrates such as amphipods. Eleven samples were taken from water bodies in southern Patagonia, between 46°–50°S and 68°–72°W approximately in January-February 2001 and December 2011, while four samples were obtained in central Patagonia (~44°S, 69°W) in February 2004. The samples were collected with a 100 μm-mesh size plankton net and preserved with absolute ethanol, while the EC of the sampled water bodies was measured in situ. The ostracods present in the samples were handpicked with a pipette or brush under stereomicroscope using a Bogorov sorting chamber, and stored in commercial 96% ethanol.

A third set of eight sediment samples obtained from southern Patagonia between 2009 and 2011 (field and laboratory work described in Ramón Mercau et al., 2012), termed Subset 3 for this contribution, was also considered.

Finally, the ostracod assemblage composition and associated salinity (estimated on the basis of the reported host waters ionic composition, using the AquaChem® software as described in Ramón Mercau et al., 2012) of 10 northern and central Patagonia water bodies, studied by Cusminsky et al. (2005), was compiled and named Subset 4. As there were concerns regarding the homogeneity of the criteria used to determine the species between the latter and the present authors, only the following species were included in Subset 4: *Limnocythere rionegroensis* Cusminsky and Whatley, 1996; *L. patagonica* Cusminsky and Whatley, 1996; *Argentocypris virgata* (Cusminsky and Whatley, 1996); *Eucypris cecryphalium* Cusminsky & Whatley, 2005 (in Cusminsky et al., 2005); *Kapcypridopsis megapodus* Cusminsky & Whatley, 2005 (in Cusminsky et al., 2005); and *Newnhamia patagonica* (Vávra, 1898).

It should be noted that as the numerical method chosen to estimate the ostracod-EC calibration function focuses in individual species' occurrences instead of whole assemblages' composition, it is robust to the possible bias in the representativity of samples obtained by different methods and the bias caused by the exclusion of some species in samples from Subset 4.

Adult ostracods bearing soft parts (i.e., considered to be alive at the time of sampling) were determined at specific level based on specialized bibliography (Cusminsky and Whatley 1996; Cusminsky et al., 2005; Díaz and Martens, 2014; Karanovic, 2012; Meisch, 2000; Purper and Würdig, 1974 and Rossetti and Martens, 1998); taxonomic details will be presented elsewere.

Species abundances were expressed as percentages. The four subsets described above were used to compile an initial data set

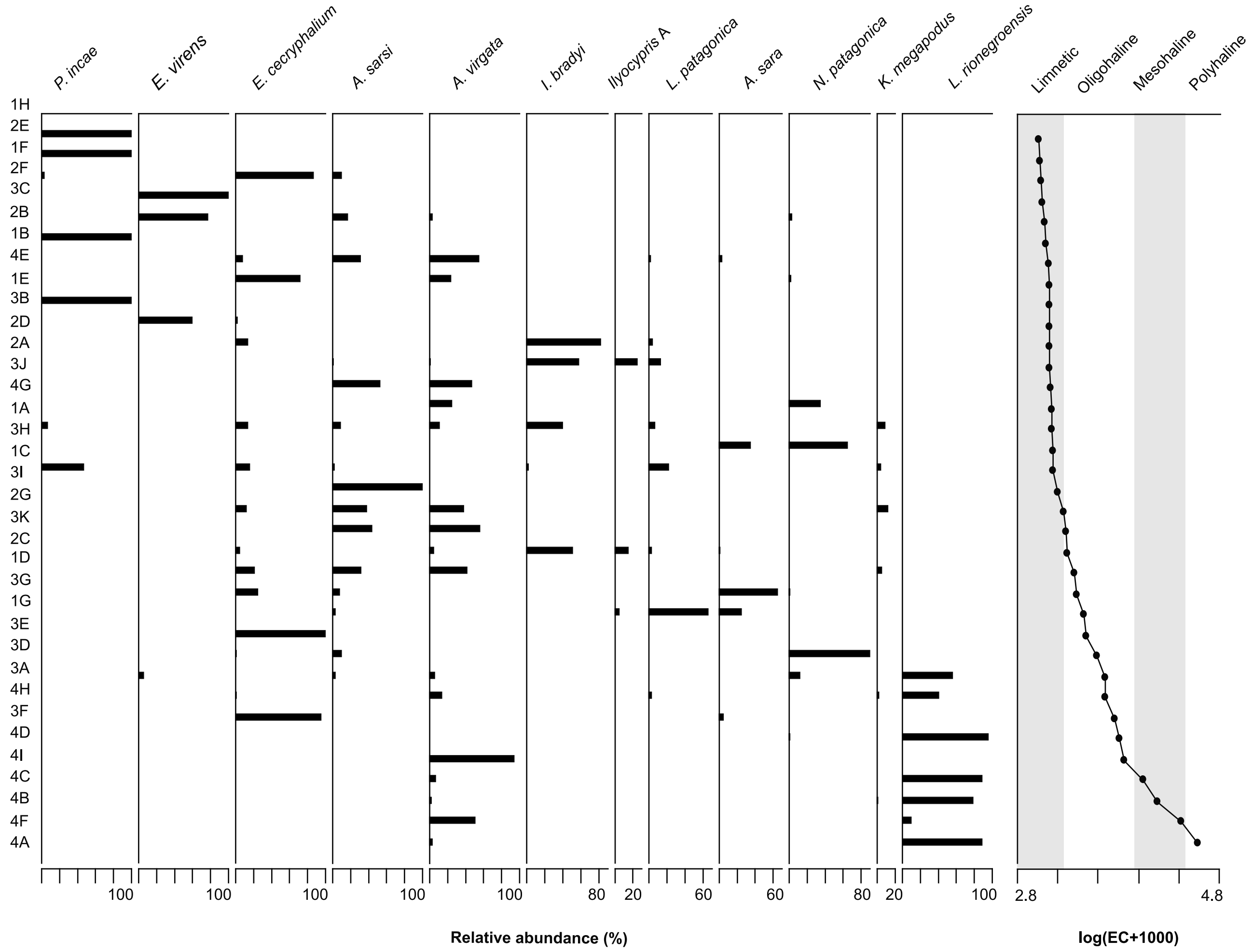

Fig. 2. Relative frequency diagram of ostracod species distribution across the dataset. Sample codes as in Table A1 of the Appendix.

($n = 44$) with the ostracod species present, their abundance and the EC (μS/cm) of their host waters. Within this composite set, only those species present on at least three samples and with relative abundance ≥3% at each one were selected to be included in the calibration set (e.g., Birks et al., 2010). This resulted in the exclusion of nine samples comprising mostly or exclusively the most infrequent species. Thus, the final calibration set ($n = 35$) consisted of the matrix $X_{35 \times 12}$ (samples × species) and the vector $Y_{35 \times 1}$ (samples × EC) (see Tables A1 and A2 of the Appendix). The Venice Symposium scale (1958, in Neale, 1988) was chosen for salinity classification; the boundaries between salinity ranges (expressed as TDS) were converted from ppm to approximate EC values (μS/cm) by applying a conversion factor of 0.64 ppm cm/μS (VIRA, 1969).

3.2. Numerical analysis and calibration

As the EC values (y) included in the calibration set span four orders of magnitude, the following logarithmic transformation was applied to the variable:

$$y' = \log(y + 1000)$$

The scale shift was selected so as to approximate the ratio between y and y' to a constant.

In order to assess the relationship between ostracod assemblage composition and EC, as well as the presence of significant secondary gradients within the calibration set, a detrended Constrained Canonical Ordination (dCCA) with detrending by segments was performed with y' as the sole explaining variable (ter Braak, 1986). No other environmental variables were recorded in all the sites in the dataset, precluding the possibility of analysing the contribution of y' in explaining the variability in ostracod assemblage composition relative to other parameters. Percentage compositional data was square-root transformed in order to stabilize its variance, and the statistical significance of the ordination was assessed by a permutation (bootstrapping) test on the first axis (999 unrestricted permutations). The fossil samples were passively added to the ordination to compare their similarity with samples in the training set. The analysis was performed using the CANOCO® 5.03 software (ter Braak and Šmilauer, 2012). The ratio of the first (constrained) axis, λ_1, with the first unconstrained axis, λ_2, was calculated in order to estimate the relative explanatory power of EC as a predictor of assemblage composition and therefore its relative importance as an ecological determinant (Juggins, 2013).

Ostracod-based conductivity calibration functions were calculated by applying weighted-averaging partial least squares (WA-PLS) regression to the calibration set using the C2 software (Juggins, 2003). Their performance was assessed in terms of the RMSEP (Root Mean Square Error of Prediction), the coefficient of determination r^2 and the maximum bias, all calculated by a leave-one-out cross-validation method. The final model and its number of components were chosen so as to maximize r^2 while minimizing

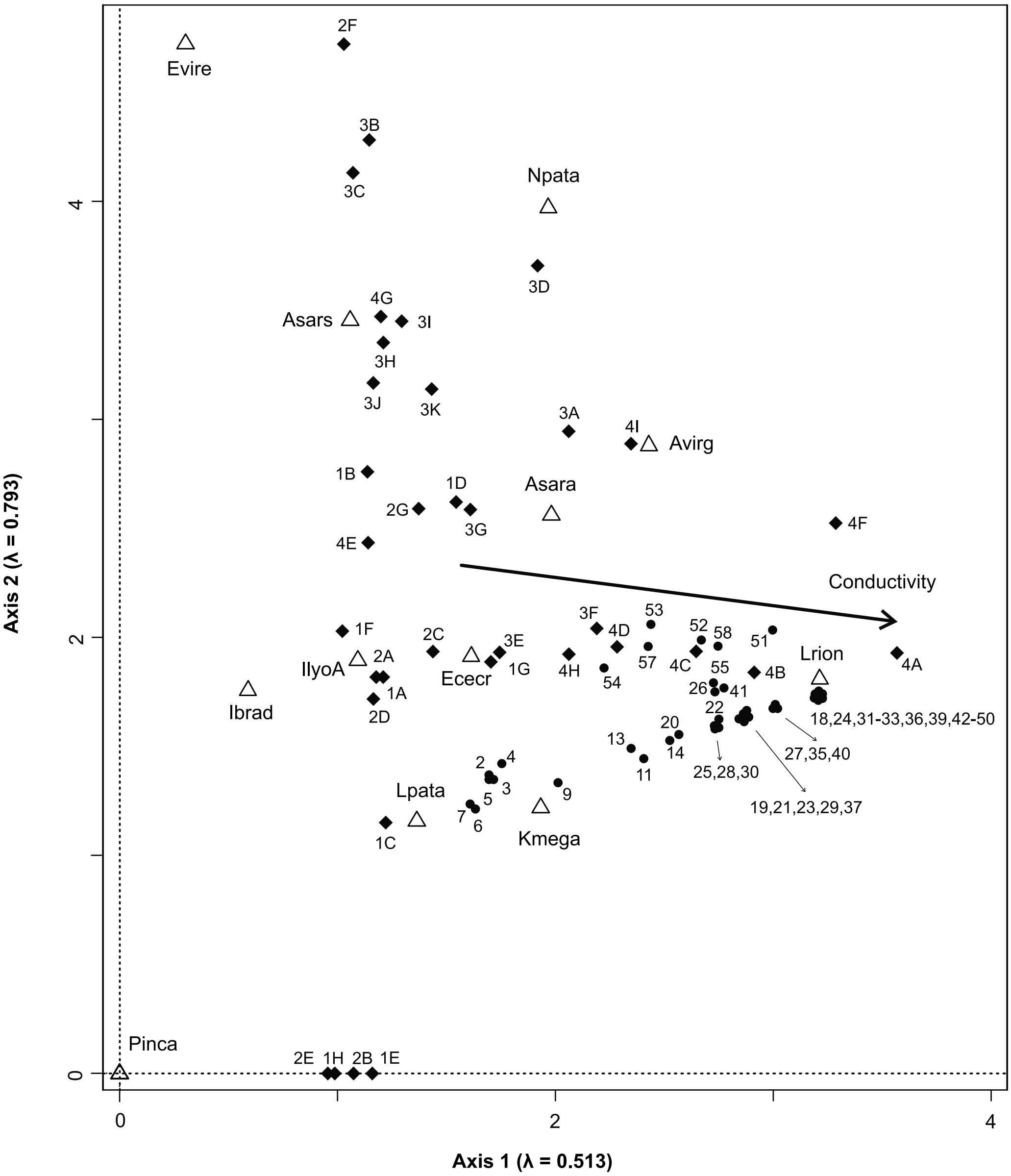

Fig. 3. First two axis of the dCCA performed on the calibration set and the fossil samples; note that only Axis 1 is canonical, as log-transformed EC (termed "Conductivity" in the plot) is the sole explaining variable. Ostracod species (empty triangles) as follows: Pinca: *Penthesilenula incae*; Lpata: *Limnocythere patagonica*; Lrion: *L. rionegroensis*; Kmega: *Kapcypridopsis megapodus*; Ececr: *Eucypris cecryphalium*; IlyoA: *Ilyocypris* A; Asars: *Argentocypris sarsi*; Asara: *A. sara*; Avirg: *A. virgata*; Npata: *Newnhamia patagonica*; Evire: *Eucypris virens*. Codes for sites (filled diamonds) in Table A1; fossil samples (filled circles) numbered according to depth.

RMSEP and maximum bias. Estimated log-transformed EC values were obtained from the calibration function for each sample of the final calibration set and plotted against the observed values of the variable, as were the residuals (estimated – observed values).

3.3. Fossil data and EC reconstruction

Fossil ostracods were recovered from sediment samples from core CHA-04/4 (58 cm), obtained from the depocentre of Laguna Cháltel. An age model based on eight radiocarbon dates was developed for the core, obtaining a basal age of 4620 cal BP (Ohlendorf et al., 2014). The core was volumetrically subsampled in continuous 1 cm intervals, resulting in multidecadal temporal resolution. Further coring, sampling and age modelling details, as well as ostracod screening procedures and species determination, are described in Ohlendorf et al. (2014), the only difference being that the latter was revised following the publication of a new Patagonian ostracod species and genus (Díaz and Martens, 2014). The species' relative abundances in the assemblages were calculated, and the calibration function was applied to this compositional data for the reconstruction of EC values.

4. Results

4.1. Calibration set

The final calibration set included 12 ostracod species. One of them could not be determined to specific level due to poor preservation of softs parts and was designated *Ilyocypris* A for the purposes of this contribution. Species richness per sample ranged from 1 to 7. Each species occurred from 3 to 17 times (median: 7) in the database, the most frequent being *A. virgata*, *A. sarsi* (Daday, 1902) and *E. cecryphalium*. Ten species presented a maximum relative abundance within the set ranging from 65% to 100%, while two – *Kapcypridopsis megapodus* and *Ilyocypris* A- were found at low relative abundances (Fig. 2).

Table 1
Performance statistics of the three first components of the WA-PLS ostracod-EC calibration function. r^2, RMSEP and maximum bias are based in a leave-one-out cross-validation method; the latter two are informed both in absolute values (on the transformed variable *y*') and as percentage of the transformed variable *y*' range (in parenthesis). The selected one-component model is shown in bold.

WA-PLS component	r^2	*Maximum bias*	*RMSEP*
1	**0.74**	**0.481 (31%)**	**0.248 (16%)**
2	0.75	0.480 (31%)	0.279 (18%)
3	0.75	0.489 (31%)	0.295 (19%)

With regards to the environmental variable, the calibration set covered a wide range of EC values (36–37,100 μS/cm; mean: 3618 μS/cm). The majority of the samples presented low and medium-low EC (median: 570 μS/cm), with 18 samples within the limnetic range (EC < 780 μS/cm), 13 oligohaline samples (780–7800 μS/cm), three samples within mesohaline values (7800–28,000 μS/cm) and only one sample within the polyhaline range (EC > 28,000 μS/cm) (Fig. 2; Table A1). The dCCA performed on the calibration set showed that log-transformed EC was statistically significant ($p = 0.002$) in explaining part of the variability in the assemblages' composition, accounting for 11.4% of it (Fig. 3). The ratio λ_1/λ_2 was 0.65.

4.2. *Fossil data*

Ostracods were present in 48 out of the 58 samples into which core CHA-04/4 was divided. Following the reappraisal of species determination, the individuals that had been assigned to *Eucypris fontana* were adscribed to *Argentocypris sarsi* and *A. sara* Díaz and Martens, 2014; thus, a total of seven species –all of which were included in the calibration set- were recognized in the fossil record. The same is dominated by *Limnocythere rionegroensis* and *L. patagonica*, which present 42 and 31 occurrences respectively, the former with a maximum abundance of 100% and the latter of 67%. The fossil samples from the upper part of the sediment core bear the least resemblance to the samples in the dataset, as they are codominated by *K. megapodus*, one of the species found at low relative frequencies in extant samples (Fig. 3).

4.3. *The EC-ostracod calibration function*

When calculating the CF on the 35 samples of the calibration set, one sample presented a very high residual value of 51% of the sampled range (one-component model; results not shown). Upon removal of this outlier sample, the second CF modelled achieved a 9% increase in r^2 and a 14% decrease in RMSEP with respect to the first one, when comparing the one-component models. The final CF selected was the one-component model of the WA-PLS regression performed on the final calibration set ($n = 34$), with $r^2 = 0.74$, RMSEP = 0.248 and maximum bias = 0.481 (16% and 31% of the sampled range, respectively). The chosen model differed from the two and three-component models mainly regarding the error estimate (Table 1).

Reconstructed log-transformed EC values in the lower part of the gradient tended to overestimate the observed ones, while reconstructed log-transformed EC values corresponding to medium and high salinities tended to be underestimated (Fig. 4). Also, the magnitude of the residuals tended to be greater for higher values (Fig. 4).

According to the calculated weighted averages, most ostracod species in the dataset presented optima at medium (oligohaline range) and low (limnetic range) salinities, while only one species, *L. rionegroensis*, presented its optimum at medium-high salinity (within the mesohaline range). The species with the lowest optima –*P. incae*, *E. virens* and *I. bradyi*- also presented the narrowest tolerance ranges, being the only species found solely within a given salinity range, whereas species with higher optima showed wider tolerance ranges (Fig. 5).

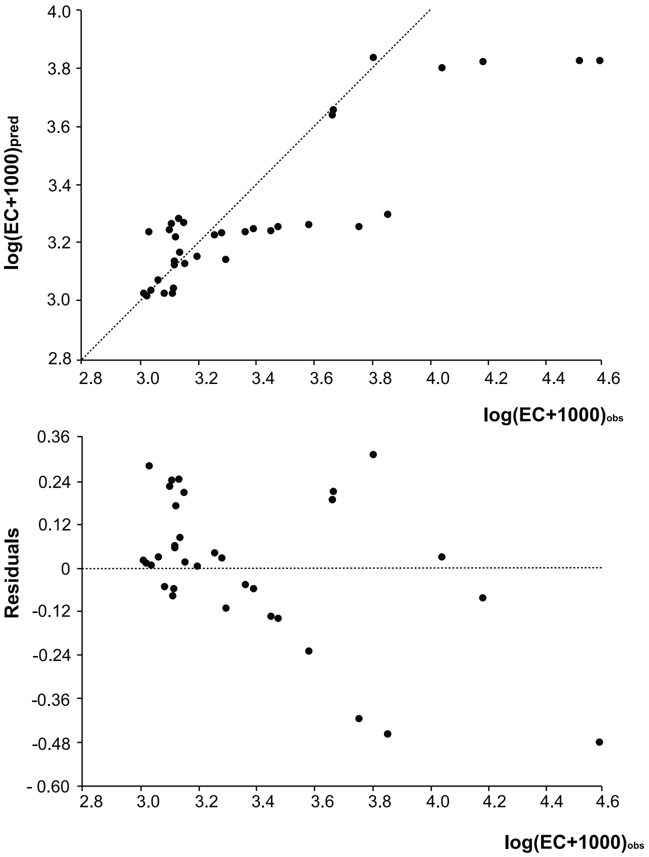

Fig. 4. Upper graph: observed vs predicted log-transformed EC; the dotted line represents the 1:1 relationship. Lower graph: observed log-transformed EC vs residuals (predicted-observed values).

4.4. *Ostracod-based reconstruction of EC values of Laguna Cháltel*

The reconstructed EC values of Laguna Cháltel range from 960 ± 70 μS/cm to 12,300 ± 740 μS/cm (Fig. 6), allowing the recognition of different phases in the record according to their variation.

In the first part of the record, from 4570 cal BP to 3990 cal BP, reconstructed EC values can be considered oligo-mesohaline and show moderate variability. The bottommost three fertile samples of the core record an increase in EC from 7100 ± 450 μS/cm at 4570 cal BP to 10,180 ± 630 μS/cm, followed by a lowering to 6400 ± 400 μS/cm at 4220 cal BP. Subsequently, EC increases, reaching a maximum of 12,300 ± 750 μS/cm at 3950 cal BP. Between 3950–2690 cal BP, the record is characterized by high, virtually constant reconstructed EC values (average: 11,570 ± 700 μS/cm); in spite of a somewhat greater variability in part of this section, for the most part the reconstructed EC values do not differ significantly.

There is a gap in the ostracod record between 2690 and 2320 cal BP, across which reconstructed EC shifts from the mesohaline (12,300 ± 750 μS/cm) to the oligohaline range (7400 ± 470 μS/cm). From 2320 cal BP to 1475 cal BP, a steep decrease in EC of approximately 5400 μS/cm is evident in spite of further discontinuities in the record. Finally, between 1060 and 230 cal BP, reconstructed EC stabilizes around an average value of 990 ± 75 μS/cm, similar to the values measured on the two sampling dates (788 μS/cm in the

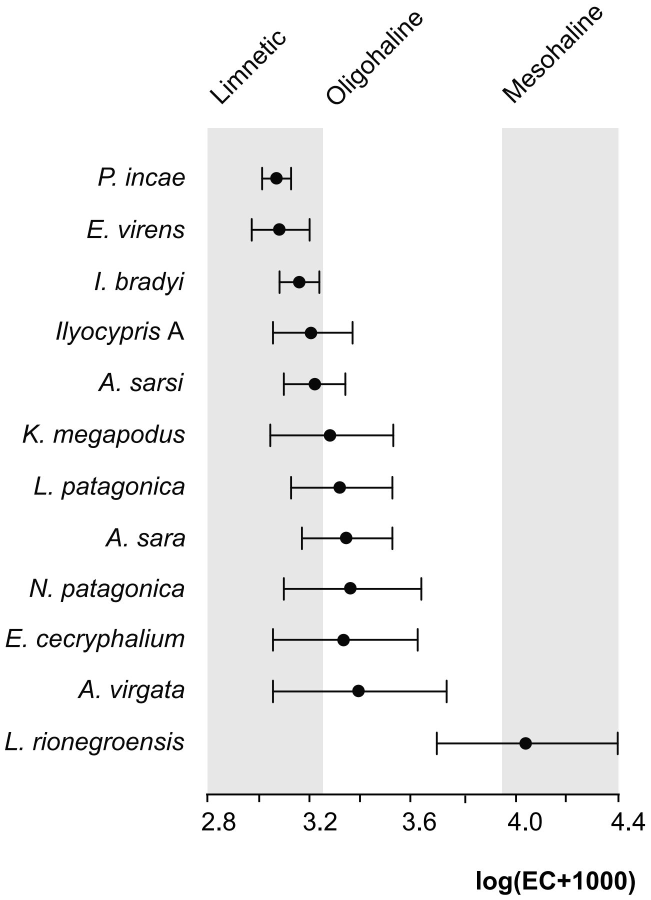

Fig. 5. Log-transformed EC optima and tolerance, estimated through weighted average, of the ostracod species included in the calibration function.

Austral summer of 2004 and 815 µS/cm in the Austral autumn of 2013; Fig. 6).

5. Discussion

5.1. Calibration function performance

The present CF shows a good performance, comparable to that of examples of similar (in terms of the calibration set size and ecological salinity ranges included) published ostracod-based CFs. Mischke et al. (2007) developed a CF for EC reconstruction by applying WA-PLS to a dataset of 96 Tibetan lakes spanning five orders of magnitude in measured EC, achieving an RMSEP of 12.4% of the sampled range and a coefficient of determination $r^2$of 0.71. For their part, Van Der Meeren et al. (2012) and Reed et al. (2012) utilized smaller calibration sets that the former authors (54 lakes in Mongolia and 52 lakes in Turkey, respectively), covering similarly large EC gradients; the Mongolian CF, developed through WA-PLS, presented an $r^2$of 0.77 and RMSEP equal to 18% of the sampled range, while the Turkish CF, developed through WA, presented an $r^2$of 0.83 and RMSEP of 10% of the sampled range. Both the $r^2$and RMSEP of the present CF, which fall within the values reported for the above studies, support its adequacy despite the relatively small size of the calibration set. The latter constitutes a potential cause of concern; optima estimated for taxa presenting few occurrences are more prone to biases and should be interpreted with caution. On the other hand, according to Juggins and Birks (2012) a calibration set consisting of approximately 30 lakes can suffice for systems dominated by a single strong environmental variable. This would be the case for the Argentinean Patagonia, were the marked longitudinal precipitations gradient can be regarded as the main factor controlling salinity through its influence in lacustrine hydrological balance (Díaz et al., 2000; Ramón Mercau et al., 2012).

The tendency of the calibration function to overestimate low conductivity values and underestimate high ones (Fig. 4), which can be partly attributed to a known artefact of the WA-PLS method (Birks et al., 2010), means that less reliance can be placed on estimations on both ends of the environmental gradient under study. This is particularly true of conductivity estimates in the mesohaline and polyhaline ranges, which were less represented in the calibration set. As discussed by Ramón Mercau et al. (2012), this sampling bias was unavoidable in spite of the effort to sample these water types, as it reflects to a great extent the unequal distribution of lakes between the more humid Andean Patagonia and the more arid Patagonian steppe.

While log-transformed EC accounts for a statistically significant portion of the total variance in the ostracod data, the value of 0.65 of the ratio λ_1/λ_2 implies that the taxa in the training set present mixed responses to the variable of interest and a second, unknown environmental gradient (Juggins, 2013). In this case, the lack of uniform limnological data for all the lakes of the dataset precludes the possibility of further exploring the contribution of log-transformed EC to the variability in ostracod distribution in relation to other environmental variables. The presence of a strong secondary gradient makes the model prone to spurious effects, which should be carefully considered when performing reconstructions. It must be noted, however, that it is unlikely that such potential effects could reach the point of surrogacy, as salinity, which has long been acknowledged to be a major driver in non-marine ostracods distribution (e.g., Neale, 1988), has direct physiological effects; that is, its importance is not derived from its influence on other variables, as would be the case of parameters such as depth. It is ecologically sound to attempt to reconstruct this variable from variations in ostracod species occurrence and abundance, and comparison of the result with the reconstruction of a related variable could help evaluate its performance beyond statistical parameters.

In the present study, such a comparison is performed against the expected trends in salinity derived from the hydrological reconstruction of Laguna Cháltel by Ohlendorf et al. (2014). These authors proposed that the lake evolved from an ephemeral system to a stable, relatively deep lake during the studied interval. Four sedimentary units, termed A–D, were recognized in the record, corresponding to four lacustrine phases: playa lake, shallow permanent lake, medium depth lake and deep lake. For the playa- and shallow lake phases, salinity is expected to increase both due to evaporative loss and runoff input, through redissolution of mineral crusts from the mudflats surrounding the water body (Eugster and Hardie, 1978; Hardie et al., 1978). As the lake deepened, during the medium depth and deep lake phases, the system would have shifted to a primarily climatic (P/E) control of salinity. Expected qualitative salinity variations are presented in Fig. 6.

5.2. Electrical conductivity and lake level fluctuation reconstructions for Laguna Cháltel

Overall, there is good agreement between the reconstructed EC values and the hydrological changes of Laguna Cháltel as inferred through a multiproxy approach by Ohlendorf et al. (2014), with high EC estimations for the part of the record corresponding to low lake level phases and a decrease in EC coincident with an inferred lake level rise (Fig. 6). However, the EC reconstruction differs somewhat with the expected tendencies for certain parts of the record.

While the EC reconstruction for Unit D, corresponding to the ephemeral lake phase, indicates generally high salinities as expected, neither their variation nor the locally low value of 6400 ± 400 µS/cm at 4220 cal BP seem to track the reconstructed lake level oscillations (Fig. 6). This could be due to the EC estimates

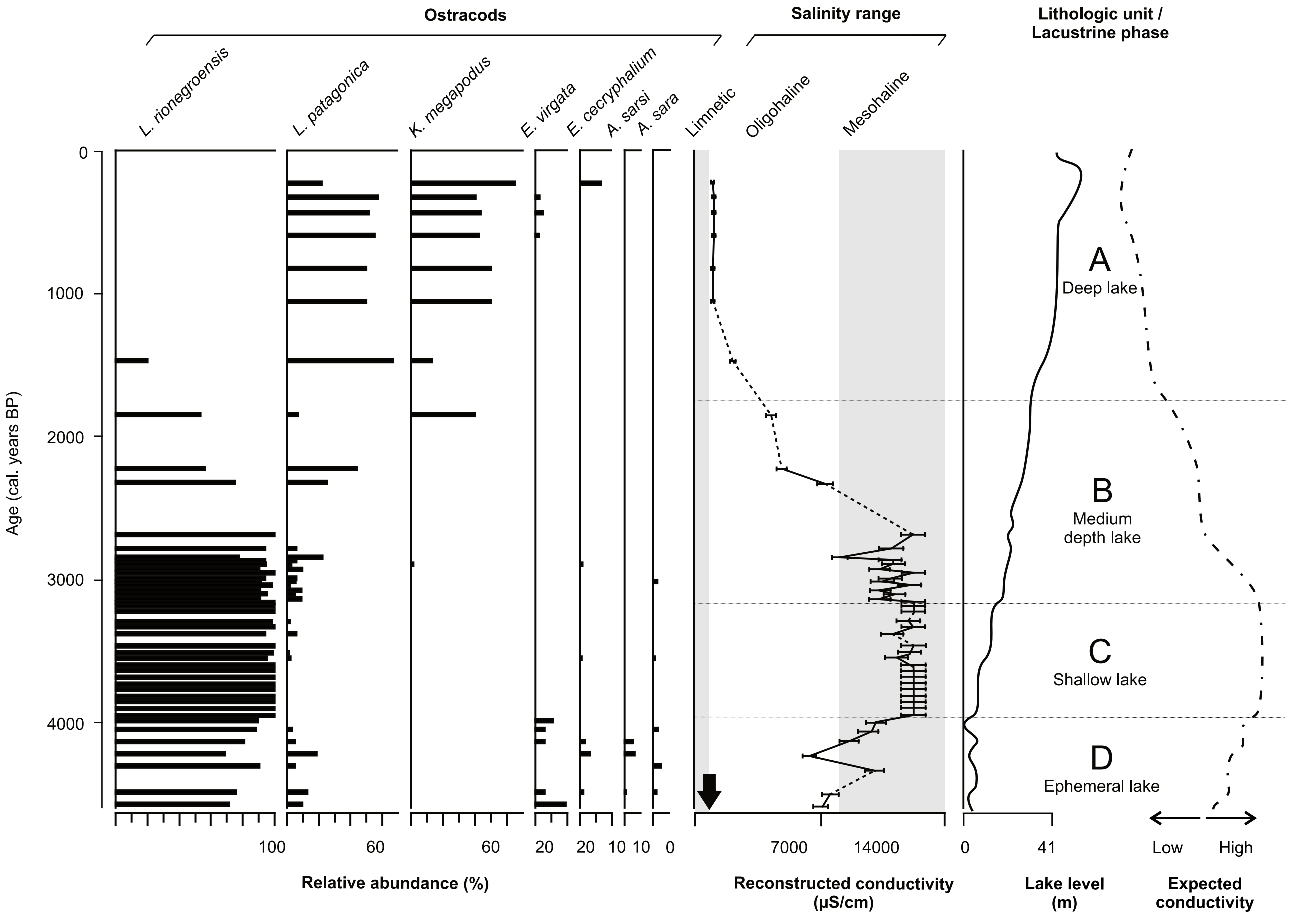

Fig. 6. Ostracod species recovered from sedimentary core CHA-04/4, reconstructed conductivity values, qualitative lake-level history of Laguna Cháltel and expected conductivity variations. The arrow over the conductivity axis shows the approximate present-day conductivity value of Laguna Cháltel, as measured in the two sampling dates (see text). Partially modified after Ohlendorf et al. (2014).

being derived from assemblages including species whose estimated optima for this variable differ by almost 9000 µS/cm (Fig. 5). These assemblages could be the result of natural post-mortem modification of ostracod community structure as a consequence of temporal mixing (e.g., Park et al., 2003) due to the low sediment accumulation rate of the lake during this phase (0.11 mm/yr; Ohlendorf et al., 2014) and an analytical time-averaging, an artifact of the need to integrate a time lapse within a single 1-cm-thick sample. Thus, each thanatocoenosis corresponds to a mixture of valves supplied by different community states or to within-habitat time averaged assemblages (Kidwell and Bosence, 1991) deposited over several decades. Therefore, the conductivity estimates actually represent averages which reflect considerable interannual/interdecadal variability. Similarly, Kemp et al. (2012) proposed that $\delta^{18}O$ values measured on a high-salinity ostracod species, *Diacypris compacta* (Herbst, 1958), were relatively heavy for a part in the record were reconstructed salinity was relatively low because *D. compacta* (recovered from fossil assemblages comprising 30–60 yr accumulation) occurred towards the end of annual/decadal cycles of evaporation and salt concentration. It is also possible that ostracods from low salinity temporal environments which could have been present in the periphery of the playa lake were transported to the water body in its centre by fluvial runoff during flooding events. Currently, small water bodies with lower ionic content (i.e., with EC in the limnetic range) than the lake can be found around it; during the 2013 sampling date, the EC measured in a small pond adjacent to the northwestern inflow to Laguna Cháltel was 140 µS/cm (Christoph Mayr, pers. comm.), while a pond located in the vicinity of the northern shore of the lake, from where Sample 13–61 was obtained, presented an EC of 97 µS/cm (Table A1).

For its part, the reconstructed increase in EC during the transition to a shallow-lake phase, in the limit between Units D and C (Fig. 6), as well as the high, constant EC values characterizing the latter, are in accordance with the independent qualitative salinity inference made by Ohlendorf et al. (2014) and the expected trend for this phase. The observed lowering of reconstructed EC values after 3190 cal BP, corresponding to the onset of Unit B, is also in agreement with independent qualitative inferences made for this part of the record. However, the decrease in EC is modest for the first part of this period, with most values falling within the mesohaline range. A considerable drop in reconstructed EC is observed between 2690 and 2320 cal BP; the onset of this freshening of the lake water as inferred through the application of the CF is uncertain, as some samples in this part of the record were devoid of ostracods. This discrepancy between expected and reconstructed values in the pace of the freshening of the lake can be reconciled if the rising lake water flooded remnants of the mudflats surrounding the water body during the first part of this phase, promoting the dissolution of salt crusts and thus countering somewhat the water dilution associated to a higher lake volume. Under this scenario, the onset of a more direct climatic control of hydrochemistry, rather than by a combination of E/P and the dissolution of salts deposited during previous lake high stands, would have taken place at some point between 2690 and 2320 cal BP, that is, at a somewhat more recent time than proposed by Ohlendorf et al. (2014). The lowering in reconstructed EC observed between ca. 1050–1850 cal BP, reaching values similar to present-day conditions, is in agreement (taking into account discontinuities in the ostracod record for this lapse) with the lake level increase which would have taken place between ca. 1200–1700 cal BP. However, a further lake level rise which would have taken place since approximately 500 cal BP is not reflected in the reconstructed EC values, which remain virtually constant from 1050 cal BP onwards. This lack of agreement could be due to the incompleteness of the ostracod record in the topmost sediments, corresponding to the proposed highest lake stand (Ohlendorf et al., 2014). While the CF can overestimate EC values in the lowest part of the gradient, the similarity in the ostracod assemblages (Fig. 6) rules out a differential bias for the individual estimates of the period in question.

6. Conclusions

The present CF achieves useful EC estimates, allowing the quantitative reconstruction of a major limnological variable in Patagonian lacustrine sedimentary records containing ostracods. While the influence of a strong secondary gradient in the dataset and the relatively small number of occurrences of some taxa could give rise to spurious effects, limiting somewhat the interpretability of the results, even a conservative application of the CF would still allow the reconstruction of broad but ecologically meaningful salinity ranges while providing an error estimate. More work is needed in order to evaluate the relative importance of other abiotic variables in Patagonian ostracods abundance and distribution, as well as their relationship with the variable of interest. For its part, further sampling of medium and high salinity lakes would enable a more accurate modelling of ostracod species response to EC in the higher part of the gradient, improving the CF's performance in terms of error estimates and maximum bias.

The good overall agreement between EC reconstructions obtained through the use of the CF and independently-derived qualitative salinity estimations for the Laguna Cháltel record evidences the robustness of the former. Moreover, the comparison between both reconstructions highlights the complex relationship between salinity, water level and climate in closed lakes. In this context, careful evaluation of CF-derived salinity reconstructions, particularly within the framework a multiproxy approach, can contribute greatly to unravel climatic and autigenic signals within a sedimentary record.

Acknowledgments

This work was supported by the following institutions: the Argentinean National Scientific and Technical Research Council (Grant D103), the Argentinean Scientific and Technical National Agency (Grant PICT/R 2006-2338), the University of Buenos Aires (grant UBACYT 20020100100999) and the German Research Foundation (DFG, Grant MA 4235/8-1). The authors wish to thank two anonymous reviewers, whose comments and suggestions greatly improved an earlier version of the present work. We are also grateful to María Cristina Marinone for making available the samples from Subset 2, which were obtained within projects funded by the following institutions: Natural Sciences and Engineering Research Council of Canada and Canada Research Chairs Program, 2000–2003; University of Buenos Aires (Grant UBACyT X-277), and the Argentinean National Scientific and Technical Research Council (Grant PIP 418). This is the IDEAN contribution number R-185.

Appendix A

Table A1
Location, temporal stability (as reported by the original authors, when applicable) and EC of the lakes included in the calibration set. The original sample names are listed, with the code used in the present study in brackets.

Subset	Sample name (code)	Latitude (°S)	Longitude (°W)	Elevation (m.a.s.l.)	Temporal stability	Electrical conductivity (μS/cm)
1	CFI (1A)	50.32	72.80	588	Permanent	370
	LALT(1B)	50.43	71.86	537	Temporary	269
	LTOR (1C)	49.58	72.35	244	Permanent	426
	LUER (1D)	51.75	72.08	157	Permanent	1299
	LSOSI (1E)	50.18	72.77	556	Temporary	292
	LNIE (1F)	49.31	72.95	742	Permanent	78
	LMOR (1G)	49.39	72.90	879	Permanent	1834
	LPAJ (1H)	51.92	71.35	115	Permanent	36
2	13-54 (2A)	49.72	72.39	260	Temporary	314
	13-37 (2B)	50.33	72.79	190	Permanent	219
	13-80 (2C)	51.02	71.78	293	Temporary	980
	13-53 (2D)	49.57	72.39	278	Permanent	313
	13-51 (2E)	49.30	72.93	757	Permanent	48
	13-61 (2F)	49.95	71.12	858	Temporary	97
	13-57 (2G)	49.95	71.12	843	Permanent	815
3	28-1-01 (3A)	51.02	70.51	190	Temporary	3600
	30-1-01 (3B)	50.10	71.85	193	Temporary	305
	146 (3C)	52.22	68.84	81	Temporary	160
	147 B (3D)	51.55	69.07	48	Temporary	2800
	2-2-01 (3E)	46.34	68.46	332	Temporary	2000
	12-7-2-04 (3F)	44.21	69.28	766	Permanent	4690
	11-7-02-04 (3G)	44.05	69.14	664	Permanent	1458
	12-12-11 (3H)	48.73	70.99	749	Permanent	420
	16-12-11-2 (3I)	48.50	71.20	885	Temporary	570
	16-12-11-9 (3J)	48.50	71.22	892	Permanent	326
	16-12-11-8 (3K)	48.51	71.20	895	Permanent	921
4	29.1.98.2 (4A)	41.23	69.47	810	Temporary	37100
	1.2.98.3 (4B)	41.17	69.43	795	Temporary	14100
	21.1.98.3 (4C)	48.51	71.58	525	Temporary	10000
	21.1.98.1 (4D)	48.41	71.59	525	Temporary	5380
	17.1.98.4 (4E)	48.52	71.23	895	Permanent	289
	18.1.98.1 (4F)	48.93	70.08	670	Permanent	25000
	17.1.98.1 (4G)	48.67	71.08	820	Permanent	363
	12/15.1.98 (4H)	48.80	71.20	276	Permanent	3640
	17.1.98.6 (4I)	48.57	71.15	887	Permanent	6140

Table A2

Matrix $X_{35\times12}$ (samples × species) of the calibration set. Species relative abundance expressed as%; names and codes of samples as in Table A1.

Subset	Sample name	*Argentocypris sarsi*	*E.ucyrpis cecryphalium*	*Eucypris virgata*	*Limnocythere patagonica*	*Argentocypris sara*	*Newnhamia patagonica*	*Penthesilenula incae*	*Ilyocypris A*	*Eucypris virens*	*Kapcypridopsis megapodus*	*Ilyocypris bradyi*	*Limnocythere rionegroensis*
1	CFI (1A)	9	14	11	7	0	0	7	0	0	9	40	0
	LALT(1B)	31	8	55	2	3	0	0	0	0	0	0	0
	LTOR (1C)	2	16	0	22	0	0	47	0	0	4	2	0
	LUER (1D)	32	21	42	0	0	0	0	0	0	5	0	0
	LSOSI (1E)	0	0	0	0	0	0	100	0	0	0	0	0
	LNIE (1F)	10	87	0	0	0	0	3	0	0	0	0	0
	LMOR (1G)	3	0	0	66	25	0	0	5	0	0	0	0
	LPAJ (1H)	0	0	0	0	0	0	100	0	0	0	0	0
2	13-54 (2A)	1	0	1	13	0	0	0	25	0	0	58	0
	13-37 (2B)	0	0	0	0	0	0	100	0	0	0	0	0
	13-80 (2C)	0	5	5	3	1	0	0	15	0	0	51	0
	13-53 (2D)	0	14	0	4	0	0	0	0	0	0	82	0
	13-51 (2E)	0	0	0	0	0	0	100	0	0	0	0	0
	13-61 (2F)	0	0	0	0	0	0	0	0	100	0	0	0
	13-57 (2G)	38	12	38	0	0	0	0	0	0	12	0	0
3	28-1-01 (3A)	3	0	6	0	0	12	0	0	6	0	0	56
	30-1-01 (3B)	0	2	0	0	0	0	0	0	60	0	0	0
	146 (3C)	17	0	3	0	0	3	0	0	77	0	0	0
	147 B (3D)	10	1	0	0	0	90	0	0	0	0	0	0
	2-2-01 (3E)	0	100	0	0	0	0	0	0	0	0	0	0
	12-7-2-04 (3F)	0	95	0	0	5	0	0	0	0	0	0	0
	11-7-02-04 (3G)	8	25	0	0	65	1	0	0	0	0	0	0
	12-12-11 (3H)	0	0	0	0	35	65	0	0	0	0	0	0
	16-12-11-2 (3I)	100	0	0	0	0	0	0	0	0	0	0	0
	16-12-11-9 (3J)	53	0	47	0	0	0	0	0	0	0	0	0
	16-12-11-8 (3K)	44	0	56	0	0	0	0	0	0	0	0	0
4	29.1.98.2 (4A)	0	0	3	0	0	0	0	0	0	0	0	89
	1.2.98.3 (4B)	0	0	2	0	0	0	0	0	0	1	0	79
	21.1.98.3 (4C)	0	0	7	0	0	0	0	0	0	0	0	89
	21.1.98.1 (4D)	0	0	0	0	0	1	0	0	0	0	0	96
	17.1.98.4 (4E)	0	72	24	0	0	2	0	0	0	0	0	0
	18.1.98.1 (4F)	0	0	51	0	0	0	0	0	0	0	0	10
	17.1.98.1 (4G)	0	0	25	0	0	35	0	0	0	0	0	0
	12/15.1.98 (4H)	0	1	14	3	0	0	0	0	0	2	0	41
	17.1.98.6 (4I)	0	0	94	0	0	0	0	0	0	0	0	0

References

Baigún, C., Marinone, M.C., 1995. Cold-temperate lakes of South America: do they fit Northern Hemisphere models? Arch. Hydrobiol. 135 (1), 23–51.

Birks, H.J.B., Heiri, O., Seppä, H., Bjune, A.E., 2010. Strengths and weaknesses of quantitative climate reconstructions based on late-quaternary biological proxies. Open Ecol. J. 3, 68–110.

Coronato, A.M., Coronato, F., Mazzoni, E., Vázquez, M., 2008. The physical geography of Patagonia and Tierra del Fuego. In: Rabassa, J. (Ed), Late Cenozoic of Patagonia and Tierra del Fuego. Developments in Quaternary Sciences 11: 13–55.

Cusminsky, G.C., Whatley, R., 1996. Quaternary non-marine ostracods from lake beds in northern Patagonia. Rev. Esp. Paleontol. 11, 143–154.

Cusminsky, G.C., Pérez, P.A., Schwalb, A., Whatley, R.C., 2005. Recent lacustrine ostracods from Patagonia, Argentina. Rev. Esp. Micropaleontol. 37, 431–450.

Cusminsky, G.C., Schwalb, A., Pérez, P.A., Pineda, D., Viehberg, F., Whatley, R.C., Markgraf, V., Gilli, A., Ariztegui, D., Anselmetti, F.S., 2011. Late quaternary environmental changes in Patagonia as inferred from lacustrine fossil and extant ostracods. Biol. J. Linn. Soc. 103, 397–408.

Daday, E., 1902. Mikroskopische-Susswasserthiere aus Patagonia— Gesammelt von Dr Filippo Silvestri. Természetrajzi Füzetek 25, 20–310.

Díaz, A.R., Martens, K., 2014. On *Argentocypris sara* gen. nov., sp: nov. (Ostracoda) from the Patagonian wetlands of Argentina. Crustaceana 87 (5), 513–530.

Díaz, M., Pedrozo, F., Baccala, N., 2000. Summer classification of Southern Hemisphere temperate lakes (Patagonia, Argentina). Lakes Reserv.: Res Manage. 5, 213–229.

Díaz, M., Pedrozo, F., Reynolds, C., Temporetti, P., 2007. Chemical composition and the nitrogen-regulated trophic state of Patagonian lakes. Limnol. Ecol. Manag. Inland Waters 37 (1), 17–27.

De Deckker, P., 2002. Ostracod palaeoecology. In: Holmes, J.A., Chivas, A. (Eds.), The Ostracoda: Applications in Quaternary Research. American Geophysical Union, Washington, D.C, pp. 6–36.

Delorme, L.D., 1971. Paleoecological determinations using Pleistocene freshwater ostracodes. Bulletin du Centre de Recherches de Pau/Société Nationale des Pétroles d'Aquitaine 5, 341–347.

Eugster, H.P., Hardie, L.A., 1978. Saline lakes. In: Lerman, A. (Ed.), Lakes—Chemistry, Geology, Physics. Springer New York, New York, pp. 237–293.

Fritz, S.C., Juggins, S., Battarbee, R.W., Engstrom, D.R., 1991. Reconstruction of past changes in salinity and climate using a diatom-based transfer function. Nature 352, 706–708.

Garreaud, R., López, P., Minvielle, M., Rojas, M., 2013. Large-scale control on the Patagonian climate. J. Clim. 26, 215–230.

Gasse, F., Barker, P., Gell, P.A., Fritz, S.C., Chalie, F., 1997. Diatom-inferred salinity in palaeolakes: an indirect tracer of climate change. Quat. Sci. Rev. 16 (6), 547–563.

Gouramanis, C., Wilkins, D., De Deckker, P., 2010. 6000 years of environmental changes recorded in Blue Lake, South Australia, based on ostracod ecology and valve chemistry. Palaeogeography Palaeoclimatology Palaeoecology 297 (1), 223–237.

Hardie, L.A., Smoot, J.P., Eugster, H.P., 1978. Saline lakes and their deposits: a sedimentological approach. In: Matter, A., Tucker, M.E. (Eds.), Modern and Ancient Lake Sediments, vol. 2. Special Publication of the International Association of Sedimentologists, pp. 7–42.

Herbst, H.V., 1958. Neue Cypridae (Crustacea, Ostracoda) aus Australien: I. Zool Anz. 160, 177–192.

Juggins, S., Birks, H.J.B. 2012. Quantitative Environmental Reconstructions from Biological Data. In: Birks, J.B.H., Lotter, A.F., Juggins, S., Smol, J.P. (eds), Tracking Environmental Change Using Lake Sediments. Developments in Paleoenvironmental Research 5: 431–494.

Juggins, S., 2003. C2 User Guide: Software for Ecological and Palaeoecological Data Analysis and Visualization. University of Newcastle, Newcastle-upon-Tyne, England, pp. 69.

Juggins, S., 2013. Quantitative reconstructions in palaeolimnology: new paradigm or sick science? Quat. Sci. Rev. 64, 20–32.

Karanovic, I., 2012. Recent Freshwater Ostracods of the World: Crustacea, Ostracoda, Podocopida. Springer, pp. 610.

Kemp, J., Radke, L.C., Olley, J., Juggins, S., De Deckker, P., 2012. Holocene lake salinity changes in the Wimmera, southeastern Australia, provide evidence for millennial-scale climate variability. Quat. Res. 77 (1), 65–76.

Kidwell, S.M., Bosence, D.W., 1991. Taphonomy and time-averaging of marine shelly faunas. In: Allison, P.A., Briggs, D.E.G. (Eds.), Taphonomy: Releasing the Data Locked in the Fossil Record. Plenum Press, New York, pp. 115–209.

Kilian, R., Lamy, F., 2012. A review of Glacial and Holocene paleoclimate records from southernmost Patagonia (49–55 S). Quat. Sci. Rev. 53, 1–23.

Massaferro, J., Larocque-Tobler, I., 2013. Using a newly developed chironomid transfer function for reconstructing mean annual air temperature at Lake Potrok Aike, Patagonia, Argentina. Ecol. Indic. 24, 201–210.

Mayr, C., Laprida, C., Lücke, A., Martín, R.S., Massaferro, J., Ramón Mercau, J., Wissel, H., 2015. Oxygen isotope ratios of chironomids, aquatic macrophytes and ostracods for lake-water isotopic reconstructions—results of a calibration study from Patagonia. J. Hydrol. 529 (2), 600–607.

Meisch, C., 2000. Freshwater *Ostracoda* of Western and Central Europe. In: Schwoerbel, J., Zwick, P. (Eds.), Suesswasserfauna Von Mitteleuropa 8/3. Spektru Akademischer Verlag, p. 22.

Mischke, S., Herzschuh, U., Massmann, G., Zhang, C., 2007. An ostracod-conductivity transfer function for Tibetan lakes. J. Paleolimnol. 38 (4), 509–524.

Mourguiart, P., Roux, M., 1990. A new strategy for paleolake level reconstructions: transfer function use based on ostracods. Geodynamique 5, 151–165.

Neale, J.W., 1988. Ostracods and palaeosalinity reconstruction. In: De Deckker, P., Colin, J.P., Peypouquet, J.P. (Eds.), Ostracoda in Earth Sciences. Elsevier, p. 302.

Ohlendorf, C., Fey, M., Massaferro, J., Haberzettl, T., Laprida, C., Lücke, A., Maidana, N., Mayr, C., Oehlerich, M., Ramón Mercau, J., Wille, M., Corbella, H., St-Onge, G., Schäbitz, F., Zolitschka, B., 2014. Late Holocene hydrological history inferred from the sediments of Laguna Cháltel (southeastern Argentina). Palaeogeography Palaeoclimatology Palaeoecology 411, 229–248.

Park, L.E., Cohen, A.S., Martens, K., Bralek, R., 2003. The impact of taphonomic processes on interpreting paleoecologic changes in large lake ecosystems: ostracodes in Lakes Tanganyika and Malawi. J. Paleolimnol. 30 (2), 127–138.

Paruelo, J.M., Beltrán, A., Jobbágy, E., Sala, O.E., Golluscio, R.A., 1998. The climate of Patagonia: general patterns and controls on biota. Ecol. Austral 8, 85–101.

Purper, I., Würdig, N.L., 1974. Occurrence of *Heterocypris incongruens* (Ramdhor) Ostracoda in Rio Grande do Sul, Brazil. Discussion of the Allied Genera: *Cyprinotus*, *Eucypris*, *Heterocypris* and *Homocypris*, vol. 1. Pesquisas, pp. 69–91.

Ramón Mercau, J., Laprida, C., Massaferro, J., Rogora, M., Tartari, G., Maidana, N.I., 2012. Freshwater Patagonian ostracods and hydrochemical characteristics of Southern Patagonian lakes (Argentina): implications for paleoenvironmental reconstructions. Hydrobiologia 694, 235–251.

Reed, J.M., Mesquita-Joanes, F., Griffiths, H.I., 2012. Multi-indicator conductivity transfer functions for quaternary palaeoclimate reconstruction. J. Paleolimnol. 47 (2), 251–275.

Rossetti, G., Martens, K., 1998. Taxonomic revision of the recent and Holocene representatives of the family Darwinulidae (Crustacea, Ostracoda), with a description of three new genera. Bulletin de L'Institut Royal des Sciences Naturelles de Belgique 68, 55–110.

Schäbitz, F., Wille, M., Francois, J.-P., Haberzettl, T., Quintana, F., Mayr, C., Lücke, A., Ohlendorf, C., Mancini, V., Páez, M.M., Prieto, A.R., Zolitschka, B., 2013. Reconstruction of palaeoprecipitation based on pollen transfer functions –the record of the last 16 ka from Laguna Potrok Aike, southern Patagonia. Quat. Sci. Rev. 71, 175–190.

Smol, J.P., Birks, H.J.B., Lotter, F., Juggins, S., 2012. The march towards the quantitative analysis of palaeolimnological data. In: Birks, J.B.H., Lotter, A.F., Juggins, S., Smol, J.P. (eds), Tracking Environmental Change Using Lake Sediments. Developments in Paleoenvironmental Research 5: 3–17.

Tonello, M.S., Mancini, M.V., Seppä, H., 2009. Quantitative reconstruction of Holocene precipitation changes in southern Patagonia. Quat. Res. 72 (3), 410–420.

Van Bellen, S., Mauquoy, D., Payne, R.J., Roland, T.P., Daley, T.J., Hughes, P.D.M., Loader, N.J., Street-Perrott, F.A., Rice, E.M., Pancotto, V.A., 2014. Testate amoebae as a proxy for reconstructing Holocene water table dynamics in southern Patagonian peat bogs. J. Quat. Sci. 29, 463–474.

Van Der Meeren, T., Mischke, S., Sunjidmaa, N., Herzschuh, U., Ito, E., Martens, K., Verschuren, D., 2012. Subfossil ostracode assemblages from Mongolia—quantifying response for paleolimnological applications. Ecol. Indic. 14 (1), 138–151.

Vávra, W., 1898. Sásswasser-Ostracoden der Hamburger Magalhaensische Sammelreise 1892–1893. Naturhist. Mus. Hamburg 2 (3), 1–26.

Viehberg, F.A., Mesquita-Joanes, F., 2012. Quantitative transfer function approaches in palaeoclimatic reconstruction using Quaternary ostracods. In: Horne, D., Holmes, J., Viehberg F., Rodríguez-Lázaro, J. (eds), Ostracoda as Proxies for Quaternary Climate Change. Developments in Quaternary Sciences 17: 47–64.

ter Braak, C.J.F., Šmilauer, P., 2012. CANOCO Reference Manual and User's Guide: Software for Ordination, Version 5.0. Microcomputer Power, Ithaca, USA, pp. 496.

ter Braak, C.J.F., 1986. Canonical correspondence analysis: a new eigenvector technique for multivariate direct gradient analysis. Ecology 67 (5), 1167–1179.

VIRA—Victorian Irrigation Research and Advisory Services Committee, 1969. Quality Aspects of Farm Water Supplies. Report prepared by Victorian Irrigation Research and Advisory Services Committee, Melbourne44.